Inorganic Chemistry

Article

pubs.acs.org/IC

Characterization of DMSO Coordination to Palladium(II) in Solution and Insights into the Aerobic Oxidation Catalyst, $Pd(DMSO)_2(TFA)_2$

Tianning Diao, Paul White, Ilia Guzei, and Shannon S. Stahl*

Department of Chemistry, University of Wisconsin - Madison, 1101 University Avenue, Madison, Wisconsin 53706, United States

Supporting Information

ABSTRACT: Recent studies have shown that $Pd(DMSO)_2(TFA)_2$ (TFA = trifluoroacetate) is an effective catalyst for a number of different aerobic oxidation reactions. Here, we provide insights into the coordination of DMSO to palladium(II) in both the solid state and in solution. A crystal structure of $Pd(DMSO)_2(TFA)_2$ confirms that the solid-state structure of this species has one *O*-bound and one *S*-bound DMSO ligand, and a crystallographically characterized mono-DMSO complex, *trans*-$Pd(DMSO)(OH_2)(TFA)_2$, exhibits an *S*-bound DMSO ligand. ^1H and ^{19}F NMR spectroscopic studies show that, in EtOAc and THF-d_8, $Pd(DMSO)_2(TFA)_2$ consists of an equilibrium mixture of $Pd(S\text{-}DMSO)(O\text{-}DMSO)(TFA)_2$ and $Pd(S\text{-}DMSO)_2(TFA)_2$. The *O*-bound DMSO is determined to be more labile than the *S*-bound DMSO ligand, and both DMSO ligands are more labile in THF relative to EtOAc as the solvent. DMSO coordination to Pd^{II} is substantially less favorable when the TFA ligands are replaced with acetate. An analogous carboxylate ligand effect is observed in the coordination of the bidentate sulfoxide ligand, 1,2-bis(phenylsulfinyl)ethane to Pd^{II}. DMSO coordination to $Pd(TFA)_2$ is shown to be incomplete in AcOH-d_4 and toluene-d_8, resulting in Pd^{II}/DMSO adducts with <2:1 DMSO/Pd^{II} stoichiometry. Collectively, these results provide useful insights into the coordination properties of DMSO to Pd^{II} under catalytically relevant conditions.

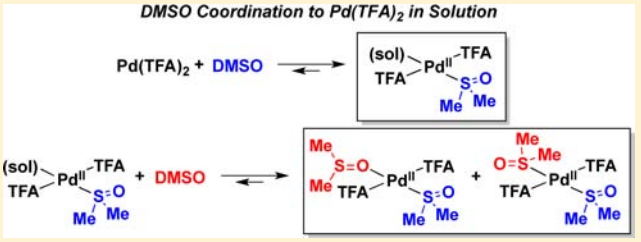

INTRODUCTION

A number of homogeneous palladium catalysts have been developed over the past decade for selective aerobic oxidation of organic molecules.[1] One of the earliest reported catalyst systems consists of $Pd(OAc)_2$ in DMSO as the solvent, which was first reported by the groups of Larock and Hiemstra in the mid-1990s.[2] This simple catalyst system has been used in a variety of oxidative transformations, including alcohol oxidation, intramolecular hetero- and carbocyclization of alkenes, and cycloalkenylation of silyl enol ethers.[3] In these reactions, DMSO has been proposed to serve as a ligand and is believed to play a vital role in stabilizing Pd^0 and promoting the reoxidation of Pd^0 by O_2.[4] Characterization of the coordination properties of DMSO in these reactions is complicated by the large excess of DMSO and insights thus far have been limited to computational studies.[5]

Sulfoxides, including DMSO and bis-sulfoxides, have been used as ligands or additives to promote a variety of Pd-catalyzed oxidation reactions, often using benzoquinone or Ag^I as the stoichiometric oxidants.[6] Recently, we have reported that $Pd(DMSO)_2(TFA)_2$, in which DMSO is present in catalytic quantities, is an effective catalyst system for a number of oxidation reactions capable of using O_2 as the oxidant, including α,β-dehydrogenation of carbonyl compounds (eq 1)[7] and oxidative amination of alkenes (eqs 2 and 3).[8] A similar catalyst system has been reported by Buchwald and co-workers for chelate-directed C−H arylation of anilides (eq 4).[9] $Pd(TFA)_2$ (TFA = trifluoroacetate) was the palladium source

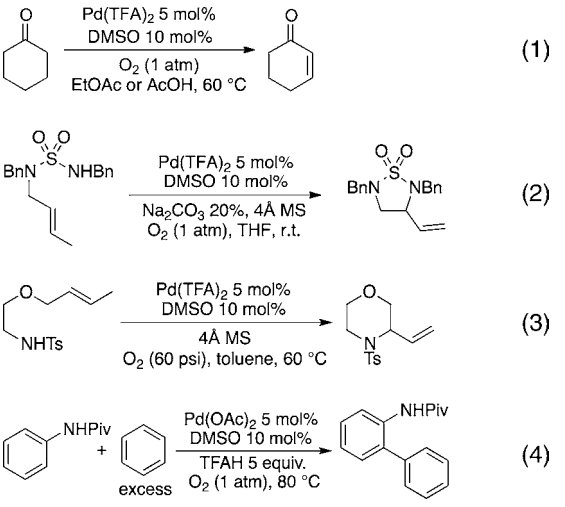

for dehydrogenation reactions and oxidative amination, while $Pd(OAc)_2$ in combination with trifluoroacetic acid was used as the catalyst in the biaryl-coupling reaction.

The coordination chemistry of DMSO to late transition metals has been the subject of considerable investigation.[10] Depending on the identity of the metal and other ancillary ligands, DMSO can exhibit *S*-, *O*-, or bridging μ-*S*,*O*-bound

Received: August 16, 2012
Published: October 23, 2012

   dx.doi.org/10.1021/ic301799p | *Inorg. Chem.* 2012, 51, 11898−11909

coordination modes. Soft metals, such as Ru^{II}, Os^{II}, Rh^{I}, and Pt^{II}, typically favor DMSO coordination via the sulfur atom, but *O*-coordination has also been observed.[10] Representative d^8 metal−DMSO complexes include $[Rh(S\text{-DMSO})_2(O\text{-DMSO})_2][PF_6]$,[11] $[Pt(bpy)(S\text{-DMSO})Cl][BF_4]$ (bpy = 2,2′-bipyridine) and $[Pd(phen)(O\text{-DMSO})Cl][PF_6]$ (phen = phenanthroline).[12] IR and ^1H NMR spectroscopic methods provide a valuable complement to X-ray crystallography in establishing the coordination mode of DMSO to transition metals.[10,13] In the aforementioned complexes, *S*-coordinated DMSO ligands exhibit S−O stretching frequencies that range from 1080 to 1154 cm^{-1}, while *O*-bound DMSO ligands exhibit lower vibrational frequencies, ranging from 862 to 997 cm^{-1} (Table 1). In the ^1H NMR spectra, *S*-bound DMSO ligands exhibit ^1H NMR chemical shifts approximately 1 ppm downfield relative to free DMSO (∼2.53 ppm), whereas *O*-bound DMSO exhibits a smaller downfield shift (Table 1).[14]

Table 1. IR and ^1H NMR Spectroscopic Data of DMSO and Transition Metal-Coordinated DMSO Reported in the Literature[10]

	IR (S−O) (cm^{-1})	^1H NMR (ppm)
free DMSO	1005	∼2.53
S-DMSO ligands	1080−1154	3.80−3.30
O-DMSO ligands	862−997	3.03−2.59

Pd^{II} complexes have been identified with both *S*- and *O*-DMSO coordination. For example, in $Pd(DMSO)_2Cl_2$ both DMSO ligands are *S*-bound,[15] whereas $[Pd(phen)(O\text{-DMSO})Cl][PF_6]$ features an *O*-bound DMSO.[12] Complexes containing both *S*- and *O*-bound DMSO ligands are also known, including $[Pd(DMSO)_4](BF_4)_2$, which has two *S*-bound and two *O*-bound DMSO ligands.[15]

$Pd(DMSO)_2(TFA)_2$ was first characterized by IR spectroscopy in the solid state in 1965 by Wilkinson and co-workers,[16] and the data provided evidence for *S*-bound DMSO. Cotton and co-workers then reported a crystal structure of this complex, which revealed the presence of *trans*-DMSO ligands, one *S*-bound and one *O*-bound.[17] In light of the growing significance of DMSO-ligated Pd^{II} complexes in aerobic oxidation reactions and the difficulty in characterizing the DMSO coordination chemistry in DMSO solvent, we wanted to establish the coordination chemistry of $Pd(DMSO)_2(TFA)_2$ in solution. Here, we report the characterization of this complex by ^1H and ^{19}F NMR spectroscopy in catalytically relevant solvents, EtOAc, THF, AcOH, and toluene. The results are supplemented by X-ray crystallographic and IR spectroscopic data, and they provide valuable insights into the structure and dynamic properties of this complex in solution.

RESULTS AND DISCUSSION

X-Ray Crystal Structures of DMSO-Ligated $Pd(TFA)_2$ Complexes. Deep-orange crystals were obtained from a solution of $Pd(TFA)_2$ and 2 equiv of DMSO in EtOAc, and X-ray diffraction analysis established the structure of *trans*-$Pd(S\text{-DMSO})(O\text{-DMSO})(TFA)_2$ (Figure 1), which exhibits only slight variations relative to the structure originally reported by Cotton and workers.[17] The *S*-bound DMSO ligand has a shorter S−O bond [1.4633(17) Å] and the *O*-bound DMSO ligand has a longer S−O bond [1.5509(16) Å] relative to that of free DMSO (1.52 Å[18]). The solid-state IR absorption spectrum of this complex reveals absorption bands at 1149 cm^{-1} and 923 cm^{-1}. These bands, which are blue- and red-shifted relative to free DMSO, ν_{S-O} = 1005 cm^{-1}, correspond to the S−O stretching frequencies of the *S*- and *O*-bound DMSO ligands, respectively.[19]

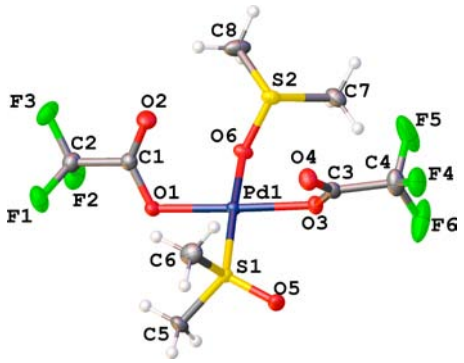

Figure 1. Molecular structure of $Pd(S\text{-DMSO})(O\text{-DMSO})(TFA)_2$, with 50% probability ellipsoids. Selected bond lengths, Å: Pd1−O1: 2.0158(15), Pd1−O3: 2.0170(16), Pd1−O6: 2.0554(16), Pd1−S1: 2.1994(5), S1−O5: 1.4633(17), S2−O6: 1.5509(16).

A mono-DMSO-ligated Pd^{II} complex was obtained from an EtOAc solution of $Pd(TFA)_2$ containing only 1 equiv of DMSO. X-ray diffraction analysis established the structure of *trans*-$Pd(S\text{-DMSO})(OH_2)(TFA)_2$ (Figure 2). The H_2O molecule, coordinated *trans* to the *S*-DMSO ligand, is hydrogen bonded to the carboxylates of adjacent molecules (see Supporting Information for details). An IR spectrum of the solid $Pd(S\text{-DMSO})(OH_2)(TFA)_2$ exhibits an absorption band at 1155 cm^{-1}, consistent with *S*-coordination of DMSO (cf. Table 1). The lack of absorption bands between 860 and 1000 cm^{-1} is consistent with the absence of an *O*-bound DMSO ligand.

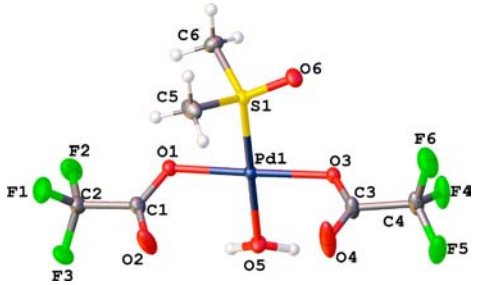

Figure 2. Molecular structure of $Pd(S\text{-DMSO})(OH_2)(TFA)_2$, with 50% probability ellipsoids. The half molecule of cocrystallized solvent ethyl acetate is not shown. Selected bond lengths, Å: Pd1−O1: 2.0205(13), Pd1−O3: 2.0171(13), Pd1−O5: 2.0564(13), Pd1−S1: 2.1979(8), S1−O6: 1.4677(13).

The Solution-Phase Structure of $Pd(TFA)_2$/DMSO in EtOAc. *(A). Spectroscopic Data.* Discrepancies can exist between solid-state and solution structures of transition-metal complexes. For example, the DMSO ligand in $[Pd(bpy)(DMSO)Cl][PF_6]$ (bpy = 2,2′-bipyridine) was determined to be *O*-bound by X-ray crystallography; however, a mixture of *O*- and *S*-DMSO ligated species was observed in CD_3NO_2 by ^1H NMR spectroscopy.[12] In order to probe the similarities and differences between solid-state and solution structures of $Pd(TFA)_2$/DMSO complexes, a combination of ^1H and ^{19}F NMR spectroscopy was used to determine the coordination properties of DMSO to Pd^{II} in catalytically relevant solvents.

dx.doi.org/10.1021/ic301799p | *Inorg. Chem.* 2012, 51, 11898−11909

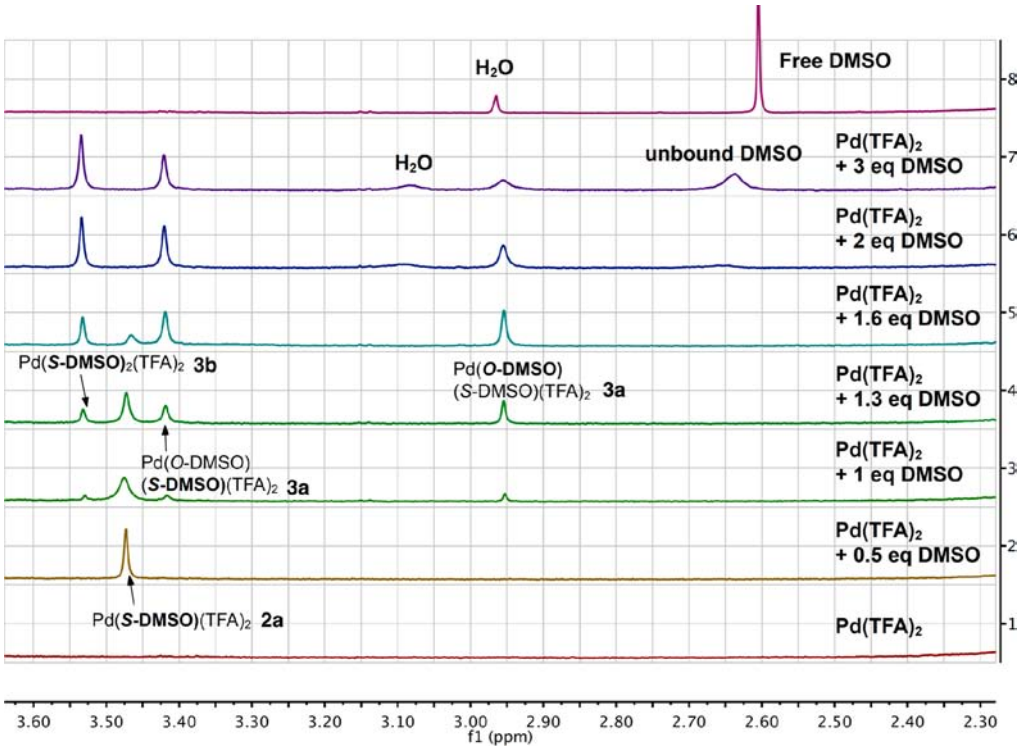

Figure 3. ^{1}H NMR spectra of $Pd(TFA)_2$ in EtOAc in the presence of various quantities of DMSO at −60 °C. Conditions: $[Pd(TFA)_2]$ = 30 mM (6.6 mg, 0.02 mmol), EtOAc = 0.65 mL, −60 °C, [DMSO] = 0, 15, 30, 39, 48, 60, and 90 mM.

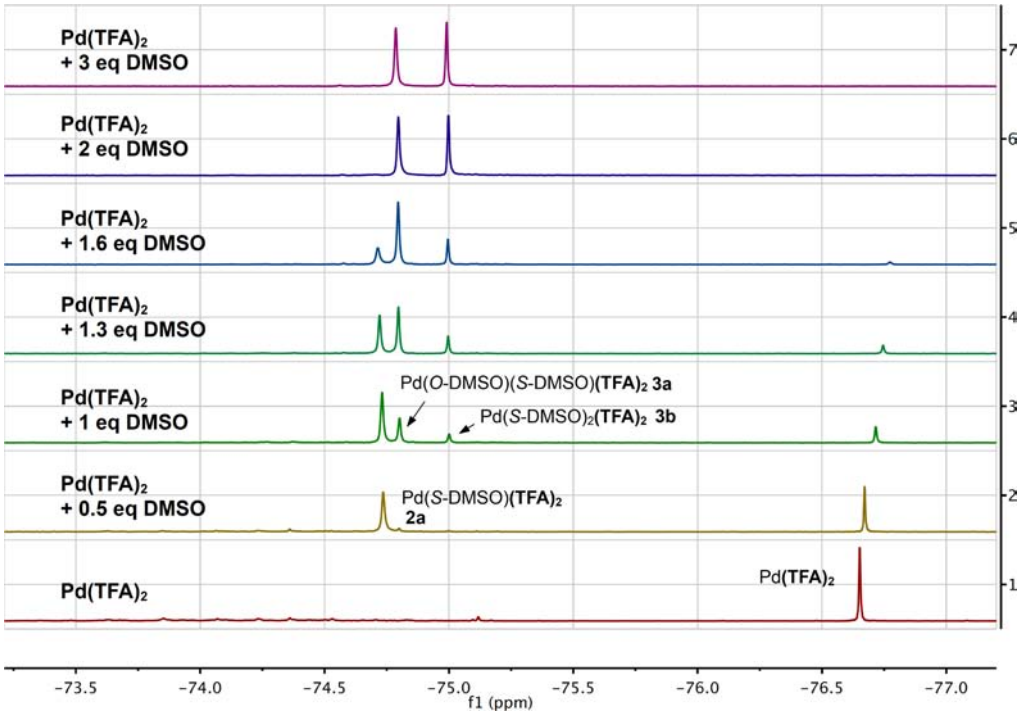

Figure 4. ^{19}F NMR spectra of $Pd(TFA)_2$ in EtOAc in the presence of various quantities of DMSO at −60 °C. Conditions: $[Pd(TFA)_2]$ = 30 mM (6.6 mg, 0.02 mmol), EtOAc = 0.65 mL, −60 °C, [DMSO] = 0, 15, 30, 39, 48, 60, and 90 mM.

The $Pd(DMSO)_2(TFA)_2$-catalyzed dehydrogenation of cyclohexanone was performed in EtOAc (eq 1), and our initial spectroscopic studies were carried out in this solvent.[7] A titration experiment was carried out by adding DMSO to a solution of $Pd(TFA)_2$ in EtOAc-d_0. The initial titration experiments were performed at −60 °C in order to slow dynamic processes. $Pd(TFA)_2$ completely dissolves in EtOAc and no ^{1}H resonances are observed in the ^{1}H NMR spectrum between 2.3 and 3.7 ppm (Figure 3). Addition of 0.5 equiv of DMSO relative to Pd results in the appearance of a singlet at 3.47 ppm. This peak grows upon addition of another 0.5 equiv of DMSO (1 equiv total), with concomitant formation of three

dx.doi.org/10.1021/ic301799p | Inorg. Chem. 2012, 51, 11898−11909

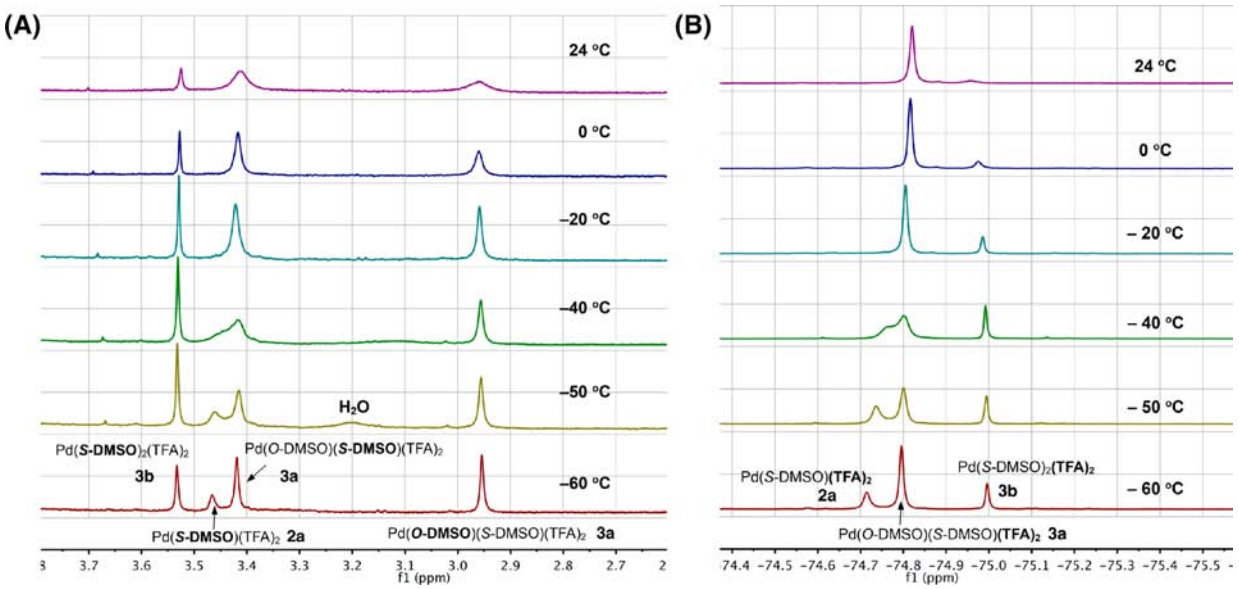

Figure 5. NMR spectra of $Pd(TFA)_2$/DMSO (1:1.6) in EtOAc at various temperatures. (A) ^1H NMR spectra; (B) ^{19}F NMR spectra. Conditions: $[Pd(TFA)_2]$ = 30 mM (6.6 mg, 0.02 mmol), [DMSO] = 48 mM (1.6 equiv), EtOAc = 0.65 mL, T = −60, −50, −40, −20, 0, and 24 °C.

new smaller peaks at 3.54, 3.42, and 2.95 ppm. Further addition of DMSO results in diminishment of the peak at 3.47 ppm and growth of the peaks at 3.54, 3.42, and 2.95 ppm. With 2 equiv of DMSO, the peak at 3.47 ppm is not present, but a new peak at 3.08 ppm is evident.[20] A broad peak, corresponding to free DMSO, appears at 2.64 ppm and the peak at 2.95 ppm is broadened in the presence of 3 equiv DMSO.

The same DMSO titration solutions were analyzed by ^{19}F NMR spectroscopy (Figure 4). In EtOAc, $Pd(TFA)_2$ exhibits a singlet at −76.76 ppm. Multiple minor species are evident between −73.50 and −75.30 ppm, the integrations of which vary at different temperatures and $Pd(TFA)_2$ concentrations. A singlet at −74.74 ppm appears upon addition of 0.5 equiv of DMSO. Further addition of DMSO leads to decreased integration of the $Pd(TFA)_2$ peak at −76.76 ppm, with concomitant growth of the peak at −74.74 ppm and appearance of two new singlets at −74.80 and −75.00 ppm. With 2 and 3 equiv of DMSO, the peaks at −74.80 and −75.00 ppm are the sole peaks present in the ^{19}F NMR spectrum.

The temperature dependence of equilibra between different $Pd(TFA)_2$/DMSO complexes has been investigated with the sample containing 1.6 equiv of DMSO, in which multiple species are evident in the NMR spectra. Both ^1H and ^{19}F NMR spectra exhibit peak broadening as the temperature is increased (Figure 5). At temperatures above −20 °C, the ^1H peaks at 3.47 and 3.42 ppm coalesce into one peak with concomitant broadening of the peak at 2.95 ppm. Similar coalescence occurs for the ^{19}F peaks at −74.74 and −74.80 ppm. In contrast, the ^1H peak at 3.54 ppm and ^{19}F peak at −75.00 ppm remain sharp throughout the temperature range.

(B). Structural Assignments. Assignments of the peaks in the ^1H NMR spectra presented above are facilitated by the literature precedents, and peaks in the ^{19}F NMR spectra may be correlated to those in the ^1H NMR spectra and assigned accordingly. The solid-state structure of $Pd(TFA)_2$ is trimeric;[21] however, Wilkinson has reported osmometry data suggesting that $Pd(TFA)_2$ dissociates into a monomer **1** in EtOAc (eq 5).[16] The peak that appears at 3.47 ppm upon addition of DMSO is assigned to an *S*-bound DMSO ligand by analogy to

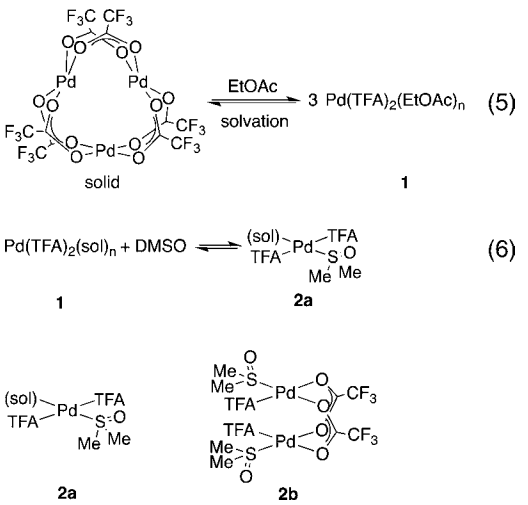

previously characterized *S*-DMSO ligands (cf. Table 1), and integration of this peak and the corresponding new TFA peak in the ^{19}F NMR spectrum at −74.74 ppm relative to an internal standard (C_6H_5F) reflects formation of a 1:1 DMSO/$Pd(TFA)_2$ complex (**2a**, eq 6), analogous to Pd(*S*-DMSO)-$(OH_2)(TFA)_2$ (cf. Figure 2). An *S*-DMSO-ligated $Pd(TFA)_2$ dimer, such as **2b**, is an alternative possible structure, particularly in light of analogous crystallographically characterized structures, $[Pd(S\text{-DMSO})(OAc)_2]_2$[22] and the phenylsulfoxide-ligated $Pd(TFA)_2$ dimer (Scheme 1).[23,24]

The peaks that appear in the ^1H and ^{19}F NMR spectra upon addition of ≥1 equiv of DMSO are consistent with bis-DMSO-

Scheme 1. Dimeric Carboxylate-Bridged Pd^{II} Complexes Reported in the Literature[22,23]

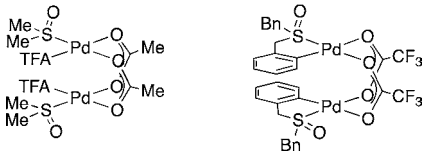

dx.doi.org/10.1021/ic301799p | *Inorg. Chem.* 2012, 51, 11898−11909

coordinated Pd species. The ^{1}H peaks at 3.54 ppm and 3.42 ppm represent two different *S*-bound DMSO ligands, whereas the peak at 2.95 ppm is consistent with an *O*-bound DMSO ligand. The ^{1}H resonances at 3.42 ppm and 2.95 ppm correlate with the peak at −74.80 ppm in the ^{19}F NMR spectra, and their respective integrations correspond to a ligand ratio of 1 *S*-DMSO/1 *O*-DMSO/2 TFA, consistent with the assignment of this species as Pd(*S*-DMSO)(*O*-DMSO)(TFA)$_2$ **3a** (eq 7). The

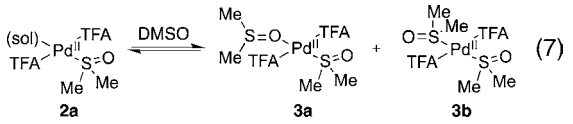

(7)

remaining *S*-bound DMSO peak at 3.54 ppm correlates with an ^{19}F peak at −75.00 ppm, and integrations of these peaks correspond to a 1:1 DMSO:TFA ligand ratio. This complex is assigned as Pd(*S*-DMSO)$_2$(TFA)$_2$ **3b**, in which both DMSO ligands coordinate via the sulfur atom (eq 7). Both *cis* and *trans* geometries of bis-(*S*-DMSO) Pd^{II} and Pt^{II} complexes are known.[25,26] Examples include *trans*-Pd(*S*-DMSO)$_2$Cl$_2$,[25b] *trans*-Pd(*S*-DMSO)$_2$(Ar)(TFA) (Ar = 2,4,5-(MeO)$_3$C$_6$H$_2$)[6d] and *cis*-Pd(*S*-DMSO)$_2$(NO$_3$)$_2$.[26b] We speculate that **3b** has a *trans* geometry because it originates from displacement of the solvent ligand in *trans*-Pd(*S*-DMSO)(sol)(TFA)$_2$ **2a**. Moreover, DFT calculations indicate that the *trans* geometry is more stable than the *cis* geometry by 2.6 kcal/mol.[27]

On the basis of the above assignments, the ^{1}H and ^{19}F NMR data can be used to plot the concentrations as a function of added DMSO (Figure 6), and the plot derived from the ^{1}H NMR spectra is in good agreement with that derived from the ^{19}F NMR spectra. To summarize the results, initial addition of DMSO results in formation of a mono-DMSO-ligated Pd(TFA)$_2$ complex with DMSO coordinated via the *S* atom. Higher concentrations of DMSO leads to conversion of this species into an equilibrium mixture of bis-DMSO-ligated Pd(TFA)$_2$ complexes **3a** and **3b**. The bis-DMSO coordination to Pd^{II} is sufficiently favored that unbound DMSO is not evident until >2 equiv of DMSO is added.

In the presence of 3 equiv of DMSO, the significant line broadening is evident for the peaks corresponding to unbound DMSO and the *O*-bound DMSO ligand in **3a**. This observation suggests that fast exchange takes place between them and further implies that the *O*-bound DMSO ligand is more labile than the *S*-bound DMSO ligand. Complementary observations are obtained from the variable-temperature spectra of Pd(TFA)$_2$ in the presence of 1.6 equiv of DMSO (Figure 5). This study reveals that **2a** and **3a** undergo fast exchange at elevated temperature (eq 8). Ligand exchange of the labile *O*-DMSO

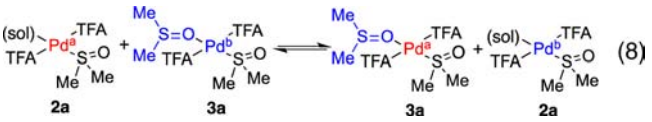

(8)

ligand in **3a** with **2a**, possibly catalyzed by the EtOAc solvent, can account for these observations. The kinetics of this exchange process will be discussed further below. The lack of peak broadening of **3b** suggests that analogous exchange of the *S*-bound DMSO ligands in **3b** does not take place on the NMR time scale.

The temperature dependence plots shown in Supporting Information (SI), Figure S8, also reveal that the concentration of **3b** decreased with concomitant increase of **3a** at increased temperature, indicating a temperature-dependent equilibrium between **3a** and **3b** (eq 9). The equilibrium constants at various

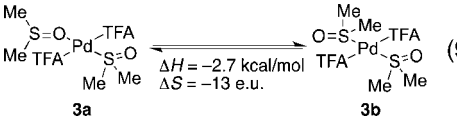

(9)

temperatures are calculated based on the ^{19}F NMR spectra. van't Hoff analysis reveals a linear relationship between the ln(K_{eq}) and 1/T (Figure S9, SI) and enables determination of ΔH and ΔS, (−2.7 kcal/mol and −13 eu, respectively). The relatively large negative ΔS suggests that **3b** has a more ordered structure than **3a**.

The catalytic oxidation of cyclohexanone in EtOAc employs Pd(TFA)$_2$ with 2 equiv of DMSO at 60 °C. The data presented above suggest that only bis-DMSO coordinated Pd compounds **3a** and **3b** are present under these conditions. At 60 °C, significant peak broadening is observed among all species (data not shown), suggesting that fast exchange can take place between both *S*- and *O*-bound DMSO ligands at this temperature. The equilibrium constant between **3a** and **3b** was calculated to be 0.17 at 60 °C, based on the van't Hoff analysis described above (eq 10). Therefore, under the catalytic conditions of dehydrogenation, **3a** is favored over **3b** by a 6:1 ratio.

Effect of the Anionic Ligand: Coordination Chemistry of DMSO to Pd(OAc)$_2$ in EtOAc. The use of trifluoroacetate as an anionic ligand is important to the success of the Pd/DMSO catalyst systems in eqs 1−3;[7,8] replacement of Pd(TFA)$_2$ with Pd(OAc)$_2$ has been shown to result in

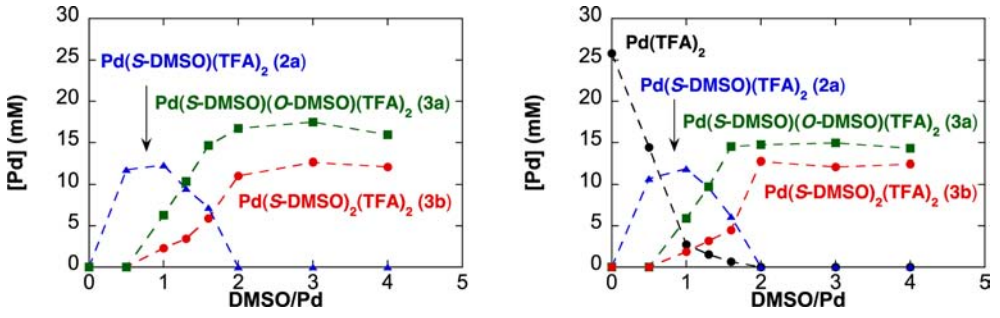

Figure 6. Concentrations of Pd(TFA)$_2$/DMSO complexes present in EtOAc as a function of added [DMSO] on the basis of ^{1}H and ^{19}F NMR data, (A) and (B), respectively. Conditions: [Pd(TFA)$_2$] = 30 mM (6.6 mg, 0.02 mmol), EtOAc = 0.65 mL, −60 °C, [DMSO] = 0, 15, 30, 39, 48, 60, and 90 mM.

dx.doi.org/10.1021/ic301799p | *Inorg. Chem.* 2012, 51, 11898−11909

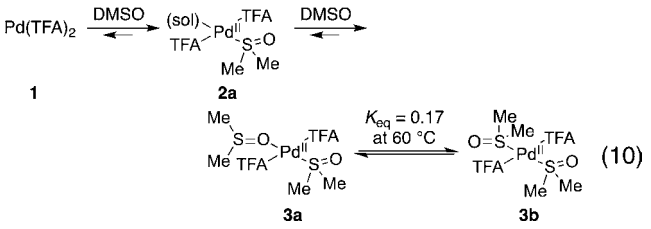

decreased yields. These observations prompted us to analyze the coordination chemistry of DMSO to $Pd(OAc)_2$ in EtOAc.

$Pd(OAc)_2$ fully dissolves in EtOAc to form an orange solution. Titration of DMSO into the solution results in the appearance of two broad peaks at 3.50 and 3.43 ppm in the ^1H NMR spectra, consistent with *S*-bound DMSO ligands, together with a peak at 2.60 ppm corresponding to free DMSO (Figure 7). Further addition of DMSO increases the

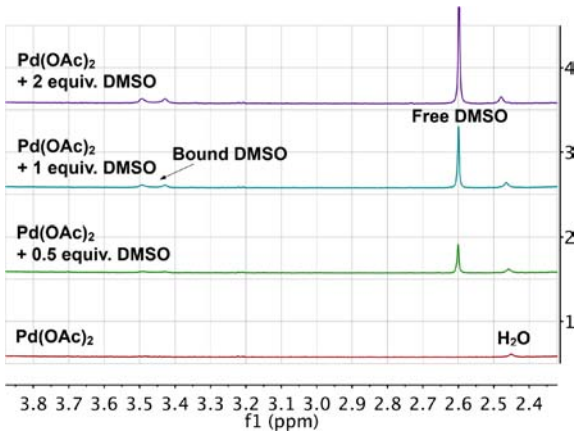

Figure 7. ^1H NMR spectra of $Pd(OAc)_2$ in EtOAc with various quantities of DMSO at 24 °C. Conditions: $[Pd(OAc)_2]$ = 30 mM (4.4 mg, 0.02 mmol), EtOAc = 0.65 mL, 24 °C, [DMSO] = 0, 7.5, 15, and 30 mM.

concentration of bound DMSO ligands; however, the sum of the bound DMSO ligands maximizes at a DMSO/Pd^{II} ratio of approximately 2:3, when ≥10 equiv of DMSO have been added (Figure 8).

The solid-state structures of $Pd(TFA)_2$ and $Pd(OAc)_2$ have both been characterized previously to be trimeric by X-ray crystallography,[21] and $Pd(OAc)_2$ has been proposed to remain trimeric in EtOAc.[16] The 2:3 DMSO:Pd^{II} stoichiometry evident from the titration experiments in Figure 8 suggests that DMSO

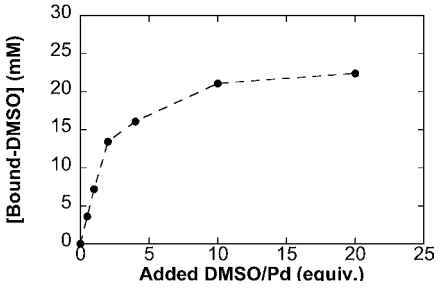

Figure 8. Titration curves of DMSO into the solution of $Pd(OAc)_2$ in EtOAc at 24 °C. Conditions: $[Pd(OAc)_2]$ = 30 mM (4.4 mg, 0.02 mmol), EtOAc = 0.65 mL, 24 °C, [DMSO] = 0, 15, 30, 60, 120, 300, and 600 mM.

coordination might partially cleave the trimeric $Pd(OAc)_2$ structure forming linear trimers, such as complexes **5a** and **5b** (eq 11). A number of structurally similar acetate-bridged

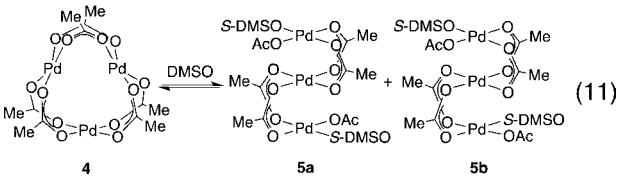

trimeric Pd complexes have been reported previously in the literature.[28] If this assignment is correct, the two distinct ^1H signals could arise from the isomeric structures, **5a** and **5b**.

Despite the tentative nature of the $Pd(OAc)_2$/DMSO structural assignments, a distinction between DMSO coordination to $Pd(TFA)_2$ and $Pd(OAc)_2$ is clearly evident. The differences presumably reflect the different basicity of the carboxylate ligands. The more basic acetate ligand should be a more effective bridging ligand, and cleavage of the trimeric structure by DMSO will be less favored. Such effects undoubtedly contribute to the different activities of $Pd(TFA)_2$ and $Pd(OAc)_2$ in the catalytic reactions. More detailed understanding of the catalytic implications of these observation will require further investigation.

The Solution-Phase Structure of $Pd(TFA)_2$/DMSO in THF-d_8. $Pd(DMSO)_2(TFA)_2$ in THF serves as an effective catalyst for oxidative amination reactions (eq 2),[8] and we performed DMSO titration experiments similar to those described above with a solution of $Pd(TFA)_2$ in THF-d_8. The spectra reveal trends similar to those observed in EtOAc, as well as differences associated with dynamics of the exchange processes (Figures 9 and 10). Addition of 0.5 equiv of DMSO leads to the appearance of a resonance at 3.29 ppm in the ^1H spectrum and a peak at −74.73 ppm in the ^{19}F NMR spectrum. These peaks are assigned to the mono-DMSO complex **2a**. Addition of more DMSO results in the appearance of peaks at 2.76 ppm and 3.35 ppm in the ^1H NMR spectra, and a peak at −74.97 ppm in the ^{19}F NMR spectra. Meanwhile, the peak at 3.29 ppm in the ^1H NMR spectra and −74.73 ppm in the ^{19}F NMR spectra shift upfield. On the basis of the analysis of the EtOAc solutions, the peak at 3.35 ppm in the ^1H NMR spectra and −74.97 ppm in the ^{19}F NMR spectra are assigned to $Pd(S\text{-}DMSO)_2(TFA)_2$, **3b**. The peak at 2.76 ppm in the ^1H NMR spectra corresponds to an *O*-bound DMSO ligand, consistent with formation of $Pd(S\text{-}DMSO)(O\text{-}DMSO)(TFA)_2$, **3a**.

The *S*-bound DMSO ligand of **3a** was not observed as an independent peak but was manifested as an upfield shift of the *S*-bound DMSO resonance of **2a**. This observation reflects fast exchange between **2a** and **3a** (cf. eq 8), resulting in coalescence of their *S*-bound DMSO resonances. Similarly, **2a** and **3a** exhibit a single broadened peak at −74.73 ppm in the ^{19}F NMR spectra. Analogous coalescence of **2a** and **3a** has been observed in EtOAc at temperatures higher than 20 °C (cf. Figure 5). When >2 equiv of DMSO are present, however, this peak appears at −74.81 ppm and is considerably sharpened, consistent with complete conversion of **2a** into **3a** (and **3b**). Complexes **2a** and **3a** do not interconvert rapidly with **3b** at −60 °C; however, when the spectra were recorded at room temperature, fast exchange was observed among all three species (**2a**, **3a**, and **3b**; Figure S13 [SI]).

The broad peak corresponding to **2a** and **3a** exhibits a chemical shift that depends on the relative concentrations of **2a**

dx.doi.org/10.1021/ic301799p | Inorg. Chem. 2012, 51, 11898−11909

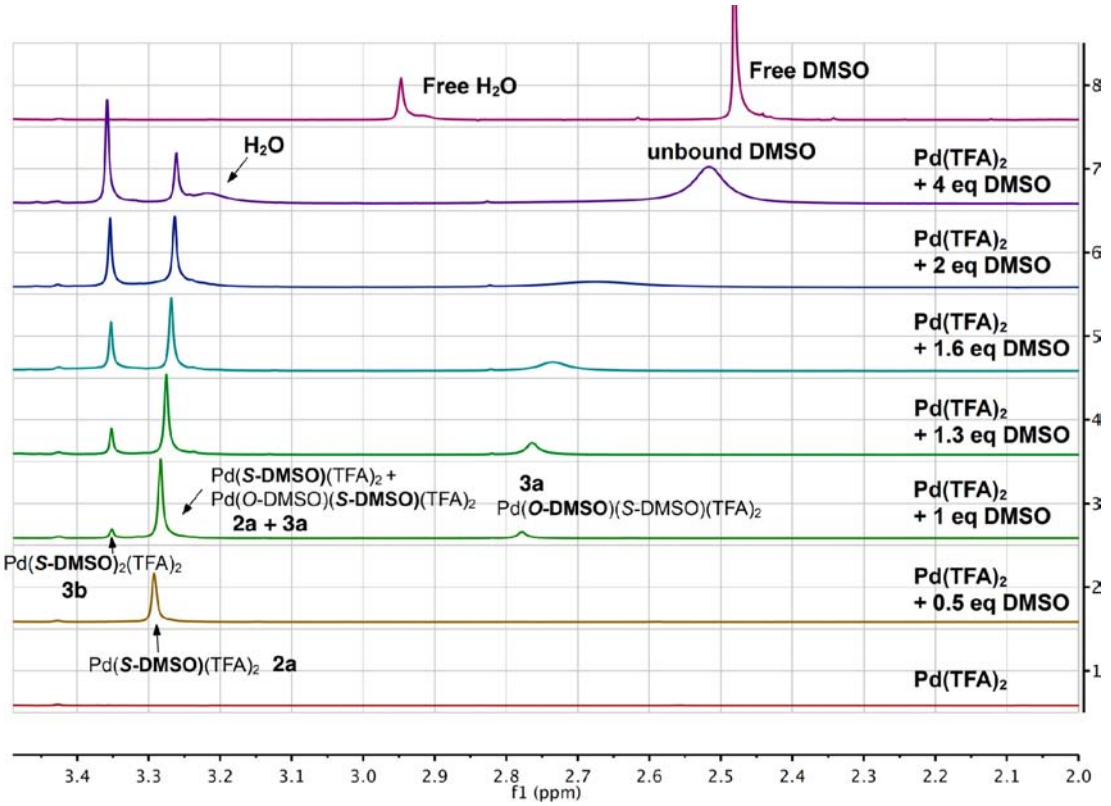

Figure 9. ^{1}H NMR spectra of $Pd(TFA)_2$ in THF-d_8 with various quantities of DMSO at −60 °C. Conditions: $[Pd(TFA)_2]$ = 15 mM (3.3 mg, 0.01 mmol), THF-d_8 = 0.65 mL, −60 °C, [DMSO] = 0, 7.5, 15, 19.5, 24, 30, and 60 mM.

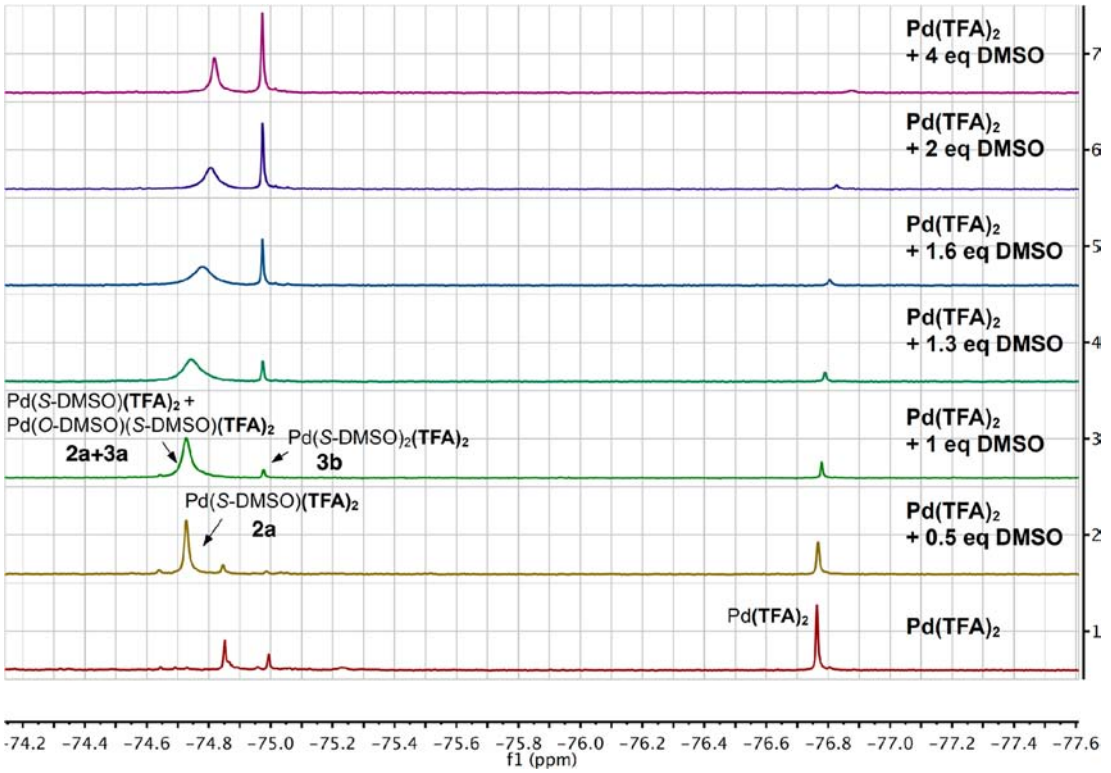

Figure 10. ^{19}F NMR spectra of $Pd(TFA)_2$ in THF-d_8 with various quantities of DMSO at −60 °C. Conditions: $[Pd(TFA)_2]$ = 15 mM (3.3 mg, 0.01 mmol), THF-d_8 = 0.65 mL, −60 °C, [DMSO] = 0, 7.5, 15, 19.5, 24, 30, and 60 mM.

and **3a**. We reasoned that with 0.5 equiv of DMSO, when **3a** has not yet started to form, the peak at 3.29 ppm in the ^{1}H NMR spectrum and −74.73 ppm in the ^{19}F NMR spectrum arise solely from **2a**. With 4 equiv of DMSO, when **2a** is

dx.doi.org/10.1021/ic301799p | Inorg. Chem. 2012, 51, 11898−11909

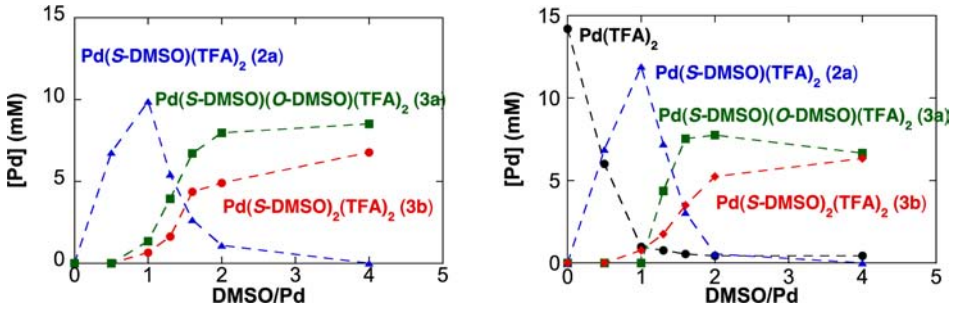

Figure 11. Titration curve of DMSO into the solution of $Pd(TFA)_2$ in THF-d_8. (A) Pd species derived from ^1H NMR spectra; (B) Pd species derived from ^{19}F NMR spectra. Conditions: $[Pd(TFA)_2]$ = 15 mM (3.3 mg, 0.01 mmol), THF-d_8 = 0.65 mL, −60 °C, [DMSO] = 0, 7.5, 15, 19.5, 24, 30, and 60 mM.

consumed, the peaks at 3.26 ppm in the ^1H NMR spectrum and −74.81 ppm in the ^{19}F NMR spectrum solely represent **3a**. The concentrations of **2a** and **3a** can be calculated on the basis of the chemical shift of the merged peaks, and the concentrations of all of the individual species are plotted as a function of added DMSO in Figure 11. In the presence of ≥2 equiv of DMSO at −60 °C, an equilibrium mixture of the two bis-DMSO coordinated Pd^{II} complexes, **3a** and **3b**, is present in very similar concentrations.

Comparison of the Kinetics of DMSO Ligand Exchange in EtOAc and THF-d_8. The interconversion between **2a** and **3a** (eq 8) resulted in line broadening of the separated peaks in EtOAc and coalescence of the peaks in THF-d_8. The rate of this process can be estimated by the peak width at half height, when the intensities of both peaks are equal.[29] At −60 °C, the concentrations of **2a** and **3a** are approximately equal when 1.3 and 1.4 equiv of DMSO are present in EtOAc and THF-d_8, respectively. The exchange rates

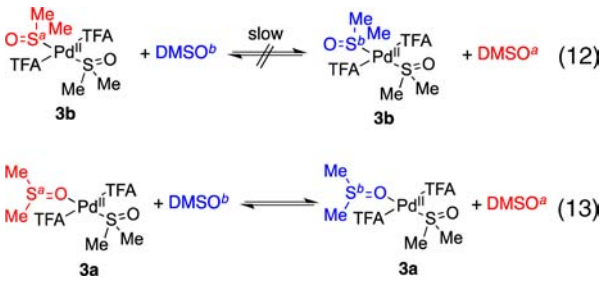

are calculated to be 3.3 s^{-1} and 116 s^{-1}, in EtOAc and THF-d_8, respectively, on the basis of the ^{19}F NMR spectra under these conditions.[30] These results, showing that ligand exchange in THF-d_8 is substantially faster than in EtOAc, can be rationalized by a solvent-catalyzed ligand exchange mechanism, in which the better coordination ability of THF[31] relative to EtOAc leads to faster exchange.[32]

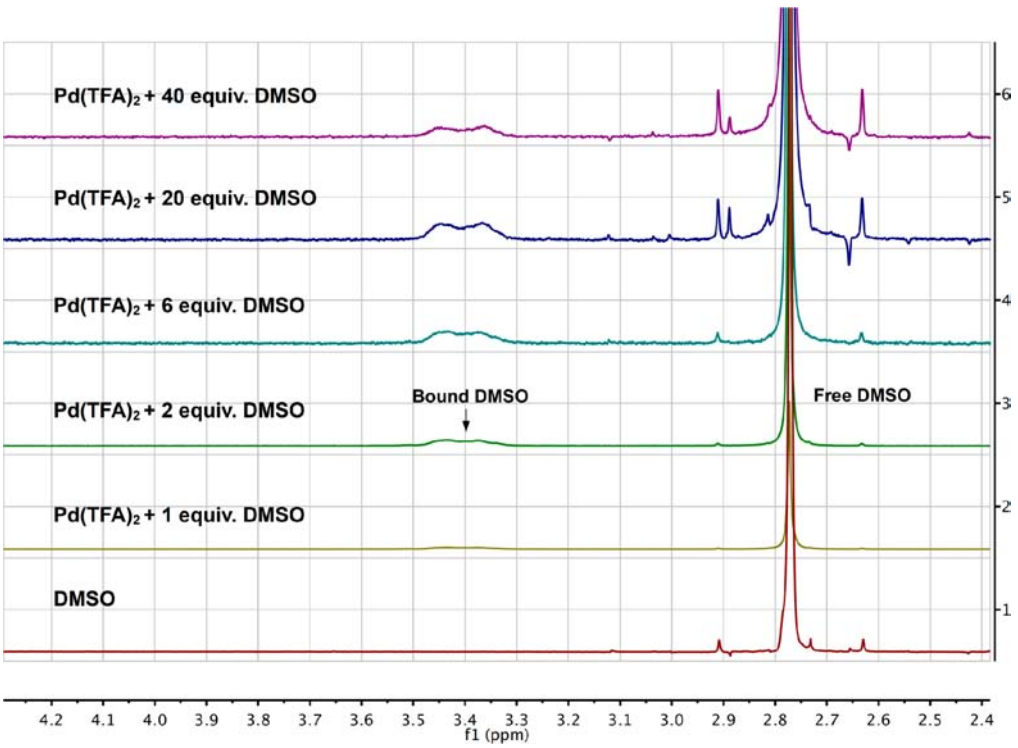

Figure 12. ^1H NMR spectra of $Pd(TFA)_2$ in AcOH-d_4 with various quantities of DMSO at 24 °C. Conditions: $[Pd(TFA)_2]$ = 15 mM (3.3 mg, 0.01 mmol), AcOH-d_4 = 0.65 mL, 24 °C, [DMSO] = 0, 15, 30, 90, 300, and 600 mM.

dx.doi.org/10.1021/ic301799p | Inorg. Chem. 2012, 51, 11898−11909

The exchange between bound and unbound DMSO was analyzed by one-dimensional (1D) NOESY saturation-transfer experiments, commonly called 1D EXSY (exchange spectroscopy).[33] When 3 equiv of DMSO are added to $Pd(TFA)_2$ in EtOAc or THF-d_8, the solutions contain a mixture of **3a**, **3b**, and unbound DMSO. The EXSY experiments performed on these solution at −60 °C reveal that saturation of the signal of **3b** does not affect other peaks. In contrast, excitation of **3a** causes inversion of the signal for the unbound DMSO (Figures S14 and S15, SI).[34] The lack of saturation transfer of **3b** to other species indicates that the DMSO ligands on **3b** are not exchanging with the unbound DMSO on the time scale of this experiment (eq 12). In contrast, the saturation transfer from **3a** to the unbound DMSO suggests that the DMSO ligand on **3a** undergoes fast exchange with the unbound DMSO (eq 13).These results have shown that the *O*-bound DMSO ligands are kinetically more labile than *S*-bound DMSO ligands. The exchange of both *O*- and *S*-bound DMSO ligands with free DMSO has been previously observed in a solution of $[Pd(bpy)(DMSO)Cl][PF_6]$ in CD_3NO_2 at 35 °C.[12]

Solution Structures of $Pd(TFA)_2$/DMSO in AcOH-d_4 and Toluene-d_8. Pd-catalyzed aerobic oxidation reactions with $Pd(TFA)_2$/DMSO catalyst systems have also been carried out in AcOH and toluene (eqs 1 and 4). NMR spectroscopic analyses of mixtures of $Pd(TFA)_2$ and DMSO suggest that DMSO coordination to Pd^{II} is not as favorable in these solvents as in EtOAc and THF (Figure 12). Upon addition of 1 equiv of DMSO to $Pd(TFA)_2$ in AcOH-d_4, unbound DMSO (2.77 ppm) is the major DMSO species, evident in the ^{1}H NMR spectrum. Smaller broad peaks present at 3.27−3.56 ppm suggest the presence of a mixture of minor *S*-bound DMSO-ligated Pd^{II} species (cf. Table 1). ^{19}F NMR spectra obtained from the titration experiments similarly exhibit a mixture of different species (Figure S17, SI). Integration of the bound DMSO peaks approaches a 1:1 DMSO:Pd stoichiometry, but only after addition of 20 equiv of DMSO (Figure 13). Possible

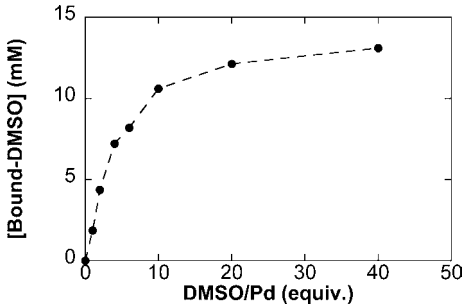

Figure 13. Titration curves of DMSO added into the solution of $Pd(TFA)_2$ in AcOH-d_4 at 24 °C. Conditions: $[Pd(TFA)_2]$ = 15 mM (3.3 mg, 0.01 mmol), AcOH-d_4 = 0.65 mL, 24 °C, [DMSO] = 0, 15, 30, 90, 300, and 600 mM.

structures consistent with a 1:1 DMSO:Pd stoichiometry include the monomeric and dimeric species **2a** and **2b** (see above). The high freezing point of AcOH-d_4 limits the utility of variable-temperature studies to gain further insights into this system.

$Pd(TFA)_2$ does not dissolve readily in toluene-d_8. Addition of 2 equiv of DMSO to the suspension of $Pd(TFA)_2$ in toluene-d_8 leads to a bright-yellow solution but does not fully dissolve $Pd(TFA)_2$. These observations indicate that DMSO coordinates to $Pd(TFA)_2$; however, a ^{1}H NMR spectrum of this suspension reveals a broad resonance in the region of free DMSO as the major species. A mixture of broad DMSO peaks approximately 0.6 ppm downfield of free DMSO supports the presence of *S*-bound DMSO ligands coordinated to Pd^{II}. Further characterization of this system was not pursued because of complications associated with the heterogeneity of this system.

Coordination of the Bidentate Sulfoxide 1,2-Bis(phenylsulfinyl)ethane to $Pd(OAc)_2$ and $Pd(TFA)_2$. Recent studies by White and co-workers have highlighted the utility of bidentate-sulfoxide ligands in $Pd(OAc)_2$-catalyzed oxidation reactions, such as allylic acetoxylation.[6c,f,g] In light of these results, we briefly investigated the coordination of 1,2-bis(phenylsulfinyl)ethane to $Pd(OAc)_2$ and $Pd(TFA)_2$ in EtOAc by ^{1}H NMR spectroscopy. The ^{1}H resonances for the phenyl group of the free 1,2-bis(phenylsulfinyl)ethane ligand appear as multiplets between 7.73 and 7.57 ppm (Figure 14).

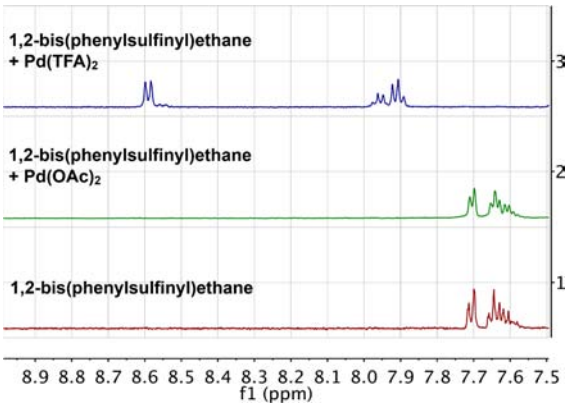

Figure 14. ^{1}H NMR spectroscopic analysis of the mixture of 1,2-bis(phenylsulfinyl)ethane with $Pd(TFA)_2$ and $Pd(OAc)_2$. Conditions: [1,2-bis(phenylsulfinyl)ethane] = 15 mM (2.7 mg, 0.01 mmol), EtOAc = 0.65 mL, 24 °C, ($[Pd(OAc)_2]$ = 15 mM), ($[Pd(TFA)_2]$ = 15 mM).

These resonances are essentially unperturbed upon addition of one equivalent of $Pd(OAc)_2$ to the solution of ligand. In contrast, substantial changes are evident when $Pd(TFA)_2$ is combined with the ligand (1:1 ratio) in EtOAc. FTIR spectra were acquired for both Pd−ligand samples upon removing the EtOAc solvent under vacuum. The IR spectra of 1,2-bis(phenylsulfinyl)ethane and of a 1:1 $Pd(OAc)_2$/1,2-bis(phenylsulfinyl)ethane mixture exhibit strong absorption bands at 1035 cm^{-1}, corresponding to the S−O stretching frequency (Figures S3 and S4, SI). These observations indicate that 1,2-bis(phenylsulfinyl)ethane does not coordinate to $Pd(OAc)_2$ in EtOAc (eq 14), and this conclusion is consistent

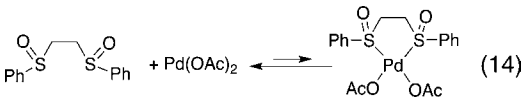

(14)

with previous studies in dichloromethane and chloroform performed by White and co-workers.[6g] In contrast, the 1:1 $Pd(TFA)_2$/1,2-bis(phenylsulfinyl)ethane mixture exhibits absorption bands at 1182 and 1148 cm^{-1} (Figure S5, SI). These blue-shifted bands are consistent with *S*-bound sulfoxide ligation.[35] No significant absorption bands are observed in the region corresponding to *O*-bound sulfoxides (1100−800 cm^{-1}). These IR data, together with the ^{1}H NMR data, show

dx.doi.org/10.1021/ic301799p | Inorg. Chem. 2012, 51, 11898−11909

that coordination of 1,2-bis(phenylsulfinyl)ethane to $Pd(TFA)_2$ is quite favorable (eq 15).

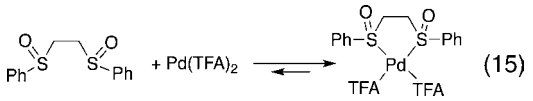

(15)

SUMMARY AND ANALYSIS

The coordination chemistry of the $Pd(TFA)_2$/DMSO catalyst system in various solvents highlights the complexity of DMSO coordination to Pd^{II} and a subtle, but potentially important, difference between the linkage−isomer coordination modes of DMSO in solution relative to the solid state. The solid-state structure of *trans*-$Pd(DMSO)_2(TFA)_2$ exhibits one *S*- and one *O*-bound DMSO ligand, whereas our solution-state studies suggest that the structure with two *S*-bound DMSO ligands is nearly isoenergetic in EtOAc and THF (cf. Figures 6 and 13). When only 1 equiv of DMSO is present, both the crystallographic and solution-phase spectroscopic data show that DMSO coordinates to Pd^{II} via the sulfur atom.

The solvent identity has a significant impact on the $Pd(TFA)_2$/DMSO coordination chemistry. In Scheme 2, the major Pd^{II} complexes formed in the presence of 2 equiv of DMSO in different solvents are highlighted in boxes. In EtOAc and THF-d_8, DMSO coordination to Pd affords an equilibrium mixture of monomeric $Pd(DMSO)_2(TFA)_2$ linkage isomers. DMSO coordinates less effectively to $Pd(OAc)_2$, relative to $Pd(TFA)_2$, and also less effectively to $Pd(TFA)_2$ in AcOH and toluene, relative to EtOAc and THF-d_8. In these cases, the substoichiometric coordination of DMSO to Pd^{II} is evident from the spectroscopic data, probably reflecting the presence of bi- or trinuclear Pd^{II}-carboxylate species that are not fully cleaved by DMSO.

Scheme 2. Summary of Solution Structures of $Pd(TFA)_2$/DMSO in Various Solvents

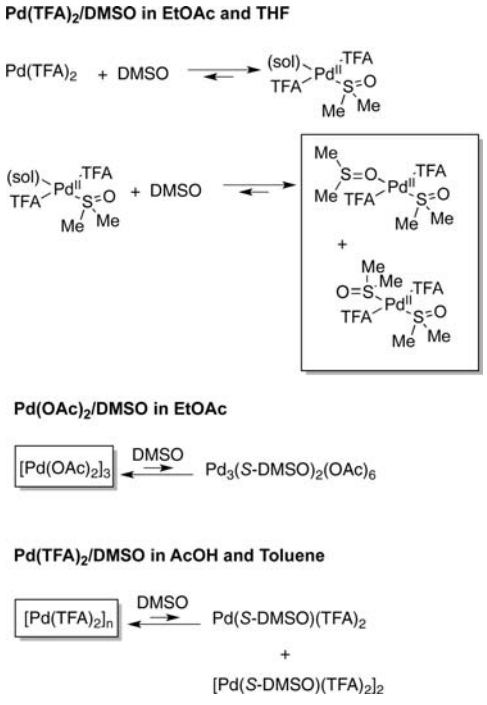

O-Bound DMSO ligands are considerably more labile than *S*-bound DMSO in $Pd(TFA)_2$/DMSO complexes. It seems reasonable that *O*- and *S*-bound DMSO ligands may work cooperatively in successful catalytic reactions. For example, a labile *O*-DMSO ligand might be important to enable weakly coordinating L-type ligands such as carbonyl oxygen atoms, alkenes, sulfonamide nitrogen atoms, and arene C−H bonds (cf. eqs 1−4) to access the coordination sphere of Pd^{II}. This insight might explain the lack of catalytic activity exhibited by $Pd(TFA)_2$ coordinated with a bidentate bis(phenylsulfinyl)-ethane ligand in dehydrogenation and oxidative amination.[7,8] This ligand chelates to Pd^{II} via the sulfur atom of the two sulfoxides.[35] On the other hand, the more-strongly coordinating *S*-DMSO ligand might be important in other steps of the catalytic mechanism. For example, the present studies do not address DMSO coordination to Pd^0; however, the "softer" character of Pd^0 relative to Pd^{II} suggests that DMSO will coordinate to Pd^0 preferentially via the sulfur atom.[5] Such coordination of DMSO to Pd^0 should stabilize the Pd^0 intermediate by inhibiting its aggregation into Pd black and facilitating oxidation of the catalyst by O_2.We speculate that the beneficial effect of DMSO in catalytic reactions carried out in AcOH and toluene might reflect this interaction of DMSO with Pd^0, despite the poor coordinating ability of DMSO to Pd^{II} in these solvents.

EXPERIMENTAL SECTION

All commercially available compounds were ordered from Sigma-Aldrich except for $Pd(TFA)_2$, which was obtained from Strem. EtOAc was purified by fractional distillation under N_2. All samples were prepared and experiments carried out in air.

^1H and ^{19}F NMR spectra were acquired on a Varian INOVA-500 MHz spectrometer. The chemical shifts (δ) of ^1H NMR spectra are given in parts per million and referenced to solvent, nondeuterated CH_3CO_2Et (2.05 ppm) and the residual C3/C4 ethylene protons of THF-d_8 (1.73 ppm). The chemical shifts (δ) in the ^{19}F NMR spectra were referenced relative to the corresponding ^1H spectra. Spectra were processed with MestReNova software. Infrared spectra were obtained with a Bruker Tensor 27 spectrometer equipped with a single reflection MIRacle Horizontal ATR ZnSe crystal by Pike Technologies.

Preparation of Pd(*S*-DMSO)(*O*-DMSO)(TFA)$_2$. Crystals of Pd(*S*-DMSO)(*O*-DMSO)$(TFA)_2$ were obtained by vapor diffusion of hexane into an EtOAc solution of $Pd(TFA)_2$ and 2 equiv of DMSO at room temperature. $Pd(TFA)_2$ (8.4 mg, 0.25 mmol) was dissolved in 0.5 mL of EtOAc, forming a deep-red solution. The solution turned bright-yellow upon addition of DMSO (3.6 μL, 0.5 mmol). This solution was filtered through glass wool into a 4 mL vial and then transferred into a 15 mL vial containing 4 mL hexane. The vial was sealed with a Teflon cap and maintained at room temperature overnight. Deep-orange crystalline needles formed.

Preparation of the Pd(*S*-DMSO)(OH$_2$)(TFA)$_2$ Complex. Crystalline Pd(*S*-DMSO)$(OH_2)(TFA)_2$ was obtained by vapor diffusion of pentane into an EtOAc solution of $Pd(TFA)_2$ and 1 equiv of DMSO at low temperature. $Pd(TFA)_2$ (8.4 mg, 0.25 mmol) was dissolved in 0.5 mL of EtOAc to form a deep-red solution. Upon addition of DMSO (1.8 μL, 0.25 mmol), the solution turned bright-yellow. The solution was filtered through glass wool into a 4 mL vial, and then transferred into a 15 mL vial containing 4 mL of pentane. The vial was sealed with a Teflon cap and placed in refrigerator at −15 °C. After 4 days, orange crystalline needles formed.

NMR Spectroscopy Study of Pd(TFA)$_2$/DMSO in EtOAc. $Pd(TFA)_2$ (6.6 mg, 0.02 mmol) was weighed into a vial, followed by injection of EtOAc (0.64 mL). The suspension transformed into a deep-red solution upon sonicating for 10 min. Fluorobenzene (4 μL, 0.041 mmol) was injected as an internal standard. The solution was transferred into an NMR tube. The spectrometer probe was precooled

dx.doi.org/10.1021/ic301799p | Inorg. Chem. 2012, 51, 11898−11909

to the desired temperature and allowed to equilibrate for 30 min. The sample was unlocked, and the ^{1}H channel was used to perform gradient shimming. A ^{1}H NMR spectrum was acquired followed by tuning the probe for ^{19}F and acquiring a ^{19}F NMR spectrum. Additional quantities of DMSO were then added from a stock solution into the same sample. The sample was allowed to mix at room temperature for 5 min and cooled to the desired temperature, and the spectrum was recorded. A longer mixing time was tested and resulted in no change of the spectrum. The volume change caused by titration was controlled to be less than 5% over the course of the experiments.

NMR Spectroscopy Study of Pd(TFA)$_2$/DMSO in THF-d_8. Pd(TFA)$_2$ (3.3 mg, 0.01 mmol) was weighed into a vial. THF-d_8 (0.64 mL) was injected to form a deep-red solution, and then fluorobenzene (4 μL, 0.041 mmol) was added as an internal standard. The solution was transferred into an NMR tube. The spectrometer probe was precooled to the desired temperature and allowed to equilibrate for 30 min. A ^{1}H NMR spectrum was acquired, followed by tuning the probe for ^{19}F and acquiring a ^{19}F NMR spectrum. Additional quantities of DMSO were then added from a stock solution into the same sample. The volume change caused by titration was controlled to be less than 5% over the course of the experiments.

This procedure was also used for the NMR spectroscopy studies of Pd(TFA)$_2$/DMSO in AcOH-d_4 and Pd(OAc)$_2$/DMSO in EtOAc.

NMR Spectroscopy Study of Pd(TFA)$_2$/DMSO in Toluene-d_8. Pd(TFA)$_2$ (3.3 mg, 0.01 mmol) was weighed out in a vial and formed a suspension with addition of toluene-d_8 (0.64 mL). Pd(TFA)$_2$ dissolved to afford a yellow solution upon addition of 2 equiv of DMSO. Fluorobenzene (4 μL, 0.041 mmol) was injected as the internal standard. The NMR spectra were acquired the same way as described above.

■ ASSOCIATED CONTENT

Ⓢ Supporting Information

Additional spectroscopic data (IR, NMR), description of dynamic NMR analysis, and an X-ray crystallographic data file. This material is available free of charge via the Internet at http://pubs.acs.org.

■ AUTHOR INFORMATION

Corresponding Author

*stahl@chem.wisc.edu

Notes

The authors declare no competing financial interest.

■ ACKNOWLEDGMENTS

We thank Lara Spencer for performing X-ray structure determinations of Figure 1. We are grateful to Dr. Charlie Fry for training and assistance with NMR experiments. Financial support of this work was provided by the NIH (R01-GM100143). Instrumentation was partially funded by the NSF (CHE-9974839, CHE-9629688, CHE-9629688, and CHE-8813550) and the NIH (1 S10 RR13866-010). Computational resources were funded, in part, by the National Science Foundation (CHE-0840494)

■ REFERENCES

(1) (a) Stahl, S. S. *Angew. Chem., Int. Ed.* **2004**, *43*, 3400−3420. (b) Stahl, S. S. *Science* **2005**, *309*, 1824−1826. (c) Gligorich, K. M.; Sigman, M. S. *Chem. Commun.* **2009**, 3854−3867. (d) Shi, Z.; Zhang, C.; Tang, C.; Jiao, N. *Chem. Soc. Rev.* **2012**, *41*, 3381−3430.

(2) (a) Larock, R. C.; Hightower, T. R. *J. Org. Chem.* **1993**, *58*, 5298−5300. (b) van Benthem, R. A. T. M.; Hiemstra, H.; Michels, J. J.; Speckamp, W. N. *J. Chem. Soc., Chem. Commun.* **1994**, 357−359.

(3) For representative examples, see refs 2a, b, and the following: (a) Rönn, M.; Bäckvall, J.-E.; Andersson, P. G. *Tetrahedron Lett.* **1995**, *36*, 7749−7752. (b) Larock, R. C.; Hightower, T. R.; Hasvold, L. A.; Peterson, K. P. *J. Org. Chem.* **1996**, *61*, 3584−3585. (c) Toyota, M.; Ihara, M. *Synlett* **2002**, *8*, 1211−1222.

(4) (a) Steinhoff, B. A.; Fix, S. R.; Stahl, S. S. *J. Am. Chem. Soc.* **2002**, *124*, 766−767. (b) Steinhoff, B. A.; Stahl, S. S. *J. Am. Chem. Soc.* **2006**, *128*, 4348−4355.

(5) Zierkiewicz, W.; Privalov, T. *Organometallics* **2005**, *24*, 6019−6028.

(6) For examples, see: (a) Grennberg, H.; Gogoll, A.; Bäckvall, J.-E. *J. Org. Chem.* **1991**, *56*, 5808−5811. (b) Bergstad, K.; Grennberg, H.; Bäckvall, J.-E. *Organometallics* **1998**, *17*, 45−50. (c) Chen, M. S.; White, M. C. *J. Am. Chem. Soc.* **2004**, *126*, 1346−1347. (d) Tanaka, D.; Romeril, S. P.; Myers, A. G. *J. Am. Chem. Soc.* **2005**, *127*, 10323−10333. (e) Hull, K. L.; Sanford, M. S. *J. Am. Chem. Soc.* **2007**, *129*, 11904−11905. (f) Chen, M. S.; Prabagaran, N.; Labenz, N. A.; White, M. C. *J. Am. Chem. Soc.* **2005**, *127*, 6970−6971. (g) Young, A. J.; White, M. C. *Angew. Chem., Int. Ed.* **2011**, *50*, 6824−6827.

(7) Diao, T.; Stahl, S. S. *J. Am. Chem. Soc.* **2011**, *133*, 14566−14569.

(8) (a) McDonald, R. I.; Stahl, S. S. *Angew. Chem., Int. Ed.* **2010**, *49*, 5529−5532. (b) Lu, Z.; Stahl, S. S. *Org. Lett.* **2012**, *14*, 1234−1237.

(9) Brasche, G.; García-Fortanet, J.; Buchwald, S. L. *Org. Lett.* **2008**, *10*, 2207−2210.

(10) For comprehensive reviews, see: (a) Calligaris, M.; Carugo, O. *Coord. Chem. Rev.* **1996**, *153*, 83−154. (b) Calligaris, M. *Coord. Chem. Rev.* **2004**, *248*, 351−375.

(11) Dorta, R.; Rozenberg, H.; Milstein, D. *Chem. Commun.* **2002**, 710−711.

(12) Annibale, G.; Cattalini, L.; Bertolasi, V.; Ferretti, V.; Gilli, G.; Tobe, M. L. *J. Chem. Soc., Dalton Trans.* **1989**, 1265−1271.

(13) (a) Price, J. H.; Williamson, A. N.; Schramm, R. F.; Wayland, B. B. *Inorg. Chem.* **1972**, *11*, 1280−1284. (b) Davies, J. A.; Hartley, F. R.; Murray, S. G. *J. Chem. Soc., Dalton Trans.* **1979**, 1705−1708.

(14) Davies, J. A. The Coordination Chemistry of Sulfoxides with Transition Metals. In *Advances in Inorganic Chemistry and Radiochemistry*; Emeléus, H. J., Sharpe, A. G., Eds.; Academic Press: New York, 1981; Vol. *24*, pp 115−187.

(15) (a) Bennett, M. J.; Cotton, F. A.; Weaver, D. L.; Williams, R. J.; Watson, W. H. *Acta Crystallogr.* **1967**, *23*, 788−796. (b) Wayland, B. B.; Schramm, R. F. *Inorg. Chem.* **1969**, *8*, 971−976. (c) Price, J. H.; Schramm, R. F.; Wayland, B. B. *J. Chem. Soc., Chem. Commun.* **1970**, 1377−1378.

(16) Stephenson, T. A.; Morehouse, S. M.; Powell, A. R.; Heffer, J. P.; Wilkinson, G. *J. Chem. Soc. (Resumed)* **1965**, 3632−3640.

(17) Bancroft, D. P.; Cotton, F. A.; Verbruggen, M. *Acta Crystallogr., Sect. C* **1989**, *45*, 1289−1292.

(18) Thomas, R.; Shoemaker, C. B.; Eriks, K. *Acta Crystallogr.* **1966**, *21*, 12−20.

(19) Forel, M.-T.; Tranquille, M. *Spectrochim. Acta A* **1970**, *26*, 1023−1034.

(20) The peak at 3.08 ppm at −60 °C (Figure 3, spectrum 6) is assigned as unbound H_2O. This assignment is supported by the increased integration upon external addition of H_2O. The chemical shift of the unbound H_2O is 0.1 ppm downfield relative to the free H_2O in the absence of Pd complexes, possibly reflecting hydrogen-bonding interactions between H_2O and the carboxylate ligands on the Pd complexes.

(21) Batsanov, A. S.; Timko, G. A.; Struchkov, Y. T.; Gerbeleu, N. V.; Indrichan, K. M.; Popovich, G. A. *Koord. Khim* **1989**, *15*, 688−693.

(22) Stash, A. I.; Perepelkova, T. I.; Kravtsova, S. V.; Noskov, Yu. G.; Romm, I. P. *Russ. J. Coord. Chem.* **1998**, *24*, 36−39.

(23) For an example of trifluoroacetate-bridged dimeric Pd sulfoxide complex, see: Rüger, R.; Rittner, W.; Jones, P. G.; Isenberg, W.; Sheldrick, G. M. *Angew. Chem., Int. Ed.* **1981**, *20*, 382−383.

(24) For related complexes with other donor ligands, see: (a) Smith, R. C.; Woloszynek, R. A.; Chen, W.; Ren, T.; Protasiewicz, J. D. *Tetrahedron Lett.* **2004**, *45*, 8327−8330. (b) Vicente, J.; Saura-Llamas, I.; Palin, M. G.; Jones, P. G.; Ramírez de Arellano, M. C. *Organometallics* **1997**, *16*, 826−833.

(25) For *trans*-(*S*-DMSO)$_2$-ligated Pd^{II} and Pt^{II} complexes, see ref 6d, , and the following: (b) Lövqvist, K. *Acta Crystallogr., Sect. C* **1996**, *52*,

1921−1924. (c) Romeo, R.; Scolaro, L. M.; Nastasi, N.; Mann, B. E.; Bruno, G.; Nicolò, F. *Inorg. Chem.* **1996**, *35*, 7691−7698.
(26) For *cis*-(*S*-DMSO)$_2$-ligated Pd^{II} and Pt^{II} complexes, see also ref 25c: (a) Johnson, B. F. G.; Puga, J.; Raithby, P. R. *Acta Crystallogr., Sect. B* **1981**, *37*, 953−956. (b) Johansson, M. H.; Oskarsson, Å. *Acta Crystallogr., Sect. C* **2001**, *57*, 1265−1267. (c) Luzyanin, K. V.; Gushchin, P. V.; Pombeiro, A. J. L.; Haukka, M.; Ovcharenko, V. I.; Kukushkin, V. Y. *Inorg. Chem.* **2008**, *47*, 6919−6930.
(27) Gas-phase geometry optimization and frequency calculations of *cis*- and *trans*-Pd(*S*-DMSO)$_2$(TFA)$_2$ were conducted with the B3LYP functional utilizing the 6-31+G* basis set for non-Pd atoms and the Stuttgart 1997 ECP/basis set for Pd within the *Gaussian09* suite of programs (complete reference is in the Supporting Information as ref 2 of section 8, **Computational Analysis of *cis*- and *trans*-Pd(*S*-DMSO)$_2$(TFA)$_2$**). The harmonic vibrational frequencies confirmed that the two geometries were minima. Single-point calculations were then performed in ethyl acetate (ε = 5.99) and tetrahydrofuran (ε = 7.43) as solvents, using the PCM solvation model with the identical basis set for Pd with an increase in the basis set for the non-Pd atoms to 6-311+G**. See Supporting Information for details.
(28) (a) Ukhin, L.Yu.; Dolgopolova, N. A.; Kuz'mina, L. G.; Struchkov, Yu. T. *J. Organomet. Chem.* **1981**, *210*, 263−272. (b) Fuchita, Y.; Takahashi, K.; Kanehisa, N.; Shinkimoto, K.; Kai, Y.; Kasai, N. *Polyhedron* **1996**, *15*, 2777−2779. (c) Moyano, A.; Rosol, M.; Moreno, R. M.; López, C.; Maestro, M. A. *Angew. Chem., Int. Ed.* **2005**, *44*, 1865−1869. (d) Giri, R.; Liang, J.; Lei, J.-G.; Li, J.-J.; Wang, D.-H.; Chen, X.; Naggar, I. C.; Guo, C.; Foxman, B. M.; Yu, J.-Q. *Angew. Chem., Int. Ed.* **2005**, *44*, 7420−7424. (e) Friedlein, F. K.; Hampel, F.; Gladysz, J. A. *Organometallics* **2005**, *24*, 4103−4105. (f) Chitanda, J. M.; Prokopchuk, D. E.; Quail, J. W.; Foley, S. R. *Organometallics* **2008**, *27*, 2337−2345. (g) Bercaw, J. E.; Day, M. W.; Golisz, S. R.; Hazari, N.; Henling, L. M.; Labinger, J. A.; Schofer, S. J.; Virgil, S. *Organometallics* **2009**, *28*, 5017−5024. (h) Vázquez-García, D.; Fernández, A.; López-Torres, M.; Rodríguez, A.; Gómez-Blanco, N.; Viader, C.; Vila, J. M.; Fernández, J. J. *Organometallics* **2010**, *29*, 3303−3307.
(29) (a) Gutowsky, H. S.; Holm, C. H. *J. Chem. Phys.* **1956**, *25*, 1228−1234. (b) Kost, D.; Carlson, E. H.; Raban, M. *J. Chem. Soc., Chem. Commun.* **1971**, 656−657.
(30) Reaction conditions for exchange-rate studies: In EtOAc, [Pd(TFA)$_2$] = 30 mM (6.6 mg, 0.02 mmol), [DMSO] = 39 mM (1.3 equiv), −60 °C. In THF-d_8, [Pd(TFA)$_2$] = 15 mM (3.3 mg, 0.01 mmol), [DMSO] = 21 mM (1.4 equiv), −60 °C.
(31) For studies of the coordinating ability of THF and the resulting effect on reactions, see: Lucht, B. L.; Collum, D. B. *Acc. Chem. Res.* **1999**, *32*, 1035−1042.
(32) Crabtree, R. H. *The Organometallic Chemistry of the Transition Metals*, 4th ed.; John Wiley & Sons: Hoboken, NJ, 2005.
(33) Claridge, T. D. W. *High-Resolution NMR Techniques in Organic Chemistry*, 2nd ed.; Elsevier Science: Oxford, 2008.
(34) See the Supporting Information for the spectra.
(35) Crystal structures of bis-sulfoxide-ligated transition-metal complexes exhibit *S*-coordination for both sulfoxides: (a) Pettinari, C.; Pellei, M.; Cavicchio, G.; Crucianelli, M.; Panzeri, W.; Colapietro, M.; Cassetta, A. *Organometallics* **1999**, *18*, 555−563. (b) Schaub, T.; Diskin-Posner, Y.; Radius, U.; Milstein, D. *Inorg. Chem.* **2008**, *47*, 6502−6512.